Pakistan Journal of Engineering and Technology, PakJET
Multidisciplinary | Peer Reviewed | Open Access
Volume: 03, Number: 03, Pages: 56- 62, Year: 2020

Investigation of Microstructure and Stress Corrosion Cracking in Al-6061-T6 Alloy at Different Loads

Muhammad Nouman[1,2,*], Aneela Wakeel[1], Zeeshan Anjum[1,3], Awais Asghar[1]

[1]Department of Metallurgy and Materials Engineering, Faculty of Mechanical and Aeronautical Engineering University of Engineering and Technology, Taxila, Punjab, Pakistan
[2]Department of Mechanical Engineering, Swedish College of Engineering and Technology, Wah Cantt
[3]Department of Mechanical Engineering, Mirpur University of Science and Technology (MUST), Mirpur Azad Kashmir

[*]Corresponding author: Muhammad Nouman (Email: engr.nouman12@gmail.com).

Abstract- **Stress corrosion cracking (SCC) refers to the damage of mechanical components which are under the combined action of static load and corrosive environment. This phenomenon occurs in various applications including naval and aerospace industry where aluminum and steel alloys experience mechanical loadings in the presence of corrosive environments. In this research work, microstructural and environmental influence on corrosion behavior of Al-6061-T6 at different static loads was investigated. A new test fixture was developed for stress corrosion cracking. Dog-bone shaped tensile specimens of Al-6061-T6 were manufactured using CNC milling machine. Tests were conducted at constant loads of 200 N, 500 N and 800 N, in three different environments: dry ambient conditions, distilled water and 3.5% NaCl solution. Testing continued for different intervals of time i.e. 96 hours, 68 hours and 4.5 hours respectively. After each set of experiments, specimens were observed for cracks using metallurgical microscope. Detailed fractographic investigation of all the tested specimens was carried out using Scanning Electron Microscope (SEM). Excessive corrosion and material degradation was observed in specimens tested in distilled water and 3.5% NaCl environments. Microstructural analysis depicted pitting corrosion and crack deformation. Some regions clearly showed that grain boundaries were attacked due to oxidation and chemical attack causing weakening of grain boundaries and resulted into intergranular corrosion. Precipitates and grain boundaries in Al-6061-T6 served as a reason of crack initiation due to hydrogen diffusion. Fractographic investigation provided the evidence of trans granular fracture as well as intergranular fracture which was observed as dimples and extensive ductile tearing.**

***Index Terms*-- Stress Corrosion Cracking, Al-6061-T6, NaCl, SEM, Fractography**

I. INTRODUCTION

Aluminum alloy is the most versatile material for various technical purposes, which is mainly due to its attractive mechanical properties including strength, low density, good formability, and high corrosion resistance [1]. Aluminum alloy, Al-6061-T6 is widely used in aircraft because of its good mechanical properties, good weldability, and excellent resistance ability against corrosion [2]. Despite the above-mentioned properties, aluminum alloys exhibit poor mechanical surface properties (such as wear resistance and microhardness) in different environments. Aluminum alloys exhibit good resistance towards corrosion because of the formation of oxide film at its surface which acts as a barrier [3] but failure of this passivation film causes the most destructive localized corrosion including pitting corrosion, crevice corrosion, intergranular corrosion, and stress corrosion [4].

Like other several materials, aluminum alloys and steels are also prone to stress corrosion cracking phenomenon. This phenomenon occurs when the materials which are prone to corrosion are under the action of static or constant loads in the presence of a corrosive environment for a considerable amount of time. The harsh corrosive environment promotes cracking [5]. In this research work, stress corrosion phenomenon was observed in Al-6061-T6 which is frequently used in marine applications. The microstructure and environmental effects on the corrosion behavior of Al-6061-T6 under different loads was investigated. A new test rig was designed for applying load and corrosive media simultaneously on tensile sample of Al-6061. This load varied in different time intervals and in different environments. Microstructure was observed through metallurgical and scanning electron microscopes (SEM).

II. LITERATURE REVIEW

Al-6061-T6 is Mg-Si based alloy of aluminum and it is primarily strengthened by the aging precipitates Mg_2Si. The precipitates such as $MgZn_2$, Mg_2Al_3, Mg_2Si and Al_2Cu etc. are formed in supersaturate solid solution during natural and artificial aging [6]. Mg_2Si and $MgZn_2$ precipitates on site may give rise to pitting corrosion. Presence of these precipitates along the grain boundaries can cause intergranular and stress corrosion cracking.

Secondary phase particles have been reported to increase the susceptibility of Al-6061-T6 towards pitting corrosion. [7]. Aluminum-magnesium alloys exhibit high corrosion resistance, easy welding, moderate mechanical strength, and processing technology which are the main reasons of its wide use in many fields including shipbuilding, automobile, and aerospace [8]. In NaCl solution, corrosion products are formed in the Al matrix. Pitting corrosion may gradually develop into intergranular corrosion with an increase in corrosion products and chloride ion concentration [9]. Corrosion is one of the biggest challenges in material functionality, and it affects the service life of materials in practical applications [10].

Micro-galvanic cell action at the grain boundaries causes intergranular cracking (IGC) in aluminum alloys. This phenomenon is associated with the precipitates, which are either more active or noble at the grain boundaries than the surrounding matrix [11]. Pitting corrosion usually occurs where these precipitates are found. Presence of these precipitates along the grain boundaries may cause intergranular and stress corrosion cracking to occur [12-15].

Investigation on the corrosive behavior of aluminum alloys in various corrosive environments has been conducted by many researchers [16]. Various corrosion phenomenon including pitting corrosion, intergranular corrosion, exfoliation corrosion and stress corrosion are found on various types of aluminum alloys [17-19]. 6061 aluminum alloy is easily corroded in a solution containing Cl ions, causing local corrosion and thereby shortening the service life [20]. Among several corrosion protection techniques applied to aluminum alloys, chromate passivation is one of the most effective surface treatments. [21].

Difference in electrochemical properties among intermetallic compound and aluminum matrix, the micro-current coupling means that pitting corrosion easily corrodes the interface between the particles and the matrix. Intermetallic phases (such as Al_2Cu and Al_3Fe) increase the corrosion rate at the grain boundaries since they act as cathodes [22]. A good resistance to stress corrosion cracking but lower mechanical strength is exhibited by the alloys in T7X condition than the T6 condition alloys [23].

The risk of reduced fatigue resistance is increased in the corrosive environment. The existences of harsh environments also accelerate the fatigue cracks. Power generation, oil and gas exploration and transportation are common examples of engineering applications which are exposed to harsh environments and changing loads [24]. Corrosion fatigue and simple mechanical fatigue are two different phenomenons due to their distinct crack growth mechanisms. During corrosion fatigue, the parts are constantly immersed in the corrosive environment, thereby ensuring that corrosive substances persistently present at the crack tip. Corrosion mechanism at the crack tip leads to material removal during corrosion fatigue while during simple mechanical fatigue, faster crack growth occurs [25]. Previous researchers who investigated the relationship between grain size and corrosion observed that as the grain size decreases, the corrosion rate also decreases to the critical size. High grain boundary density and second degradation of phase particles were reported to be the major reasons for this behavior [26].

Under combined action of stress and corrosive environment, the anodic dissolution of the grain boundary phase is more easily activated which results into fast intergranular stress corrosion cracking (IGSCC). The rate of precipitation is directly related to corrosive damage [27]. Incorporation of Cu into the grain boundary precipitates can make them less anodic and reduce the production of hydrogen at the crack tip. [28].

III. EXPERIMENTAL DETAIL

1. Material

Material under investigation in this research work was Al-6061-T651. It was purchased in the form of a rectangular sheet having thickness of 6mm as shown in **Fig. 1**. The chemical composition of this material in weight percentage is: Si 0.4-0.8, Fe 0.7, Cu 0.15-0.40, Mn 0.15, Mg 0.8-1.2, Cr 0.04-0.35, Zn 0.25, Ti 0.15.

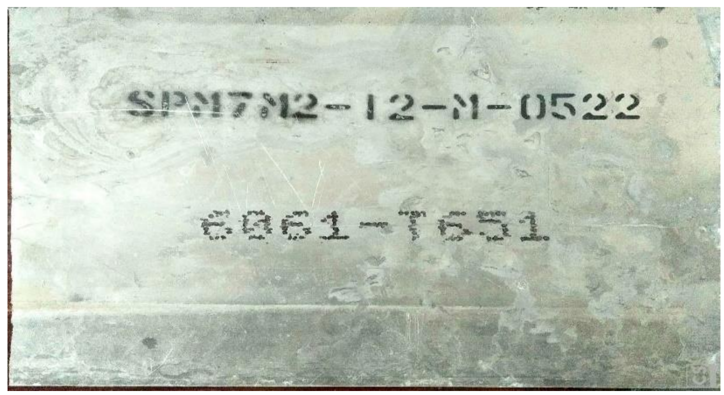

FIGURE 1: Aluminum 6061- T651 as received sheet

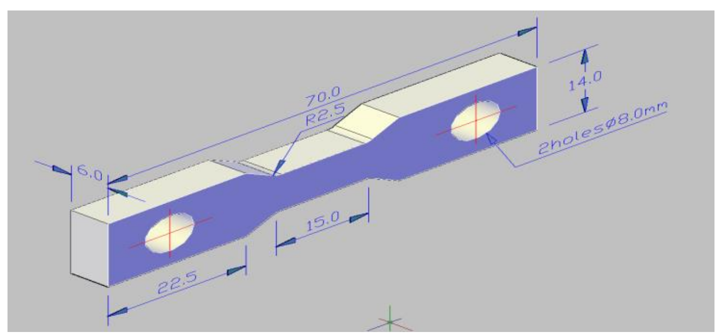

FIGURE 2: Specimen Geometry

Tensile specimens as shown in **Fig. 2** were prepared on CNC machining center according to ASTM standard (ASTM E8 / E8M-13a).

2. Experimental Setup

Three dimensional models for the newly developed test rig using CREO software has been presented in **Fig. 3**. Test rig consists of Arm, Arm pin, Base, Bearing Housing, Dead weight holder, down nut, hook, plates, lower clamp, and upper clamp as shown in **Fig. 4**. From a design perspective, height of the container was selected so that one-third of the specimen remained immersed in corrosive solution during the tests. Specimens were hanged in lower clamp with the assistance of upper clamp.

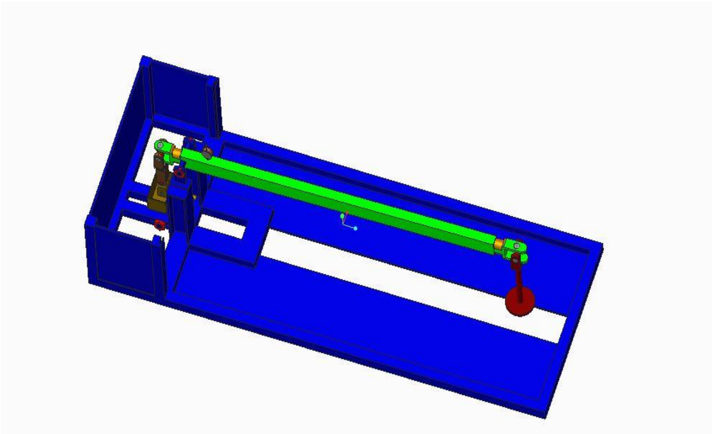

FIGURE 3: Three dimensional model of the new test rig

FIGURE 4: New test rig designed for SCC testing

3. Experimental Conditions

a. Loads

Experiments were conducted for three different static loads of 200N, 500N and 800N respectively. These loads were applied by placing weights in the hanger and load was transmitted with the help of the arm.

b. Environments

In this experimentation, specimens were tested at 03 different environments to investigate the stress corrosion cracking behavior of Aluminum 6061. Environmental effect depends upon the stress effects with respect to different intervals of time. Environments in which specimens are investigated are listed below:

- Ambient
- Distilled Water
- 3.5% NaCl Solution

FIGURE 5: a) Distilled Water b) 3.5% NaCl Solution

c. Time

All the specimens were investigated at different intervals of time. Stress and environment totally depend on time to produce appreciable stress corrosion cracking. Time of load was increased until some deformation was observed on specific load. Tests were conducted for three different time intervals as listed below:

- 96 hours
- 68 hours
- 4.5 hours

IV. RESULTS AND DISCUSSIONS

a. Structural Analysis

The micrograph of as received sample has been provided in **Fig. 6**. Structure analysis was done on the samples tested at static loading condition of 200N, 500N and 800N in three different environments such as open air, distilled water and 3.5% NaCl solution with different intervals of time i.e. 96 hours, 68 hours, 4.5 hours.

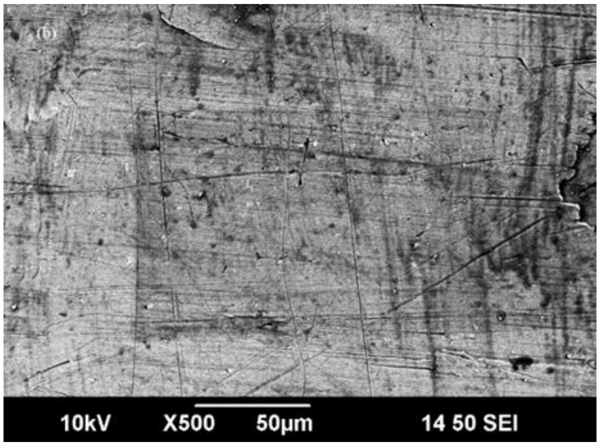

FIGURE 6: Micrograph of Al 6061, as received sample.

Figure 7 shows the sample which is dipped in 3.5M NaCl solution for 96H, this micrograph clearly shows the pitting corrosion. Similar findings were reported by the earlier researchers [29]. Sample immersed in distilled water and 3.5% NaCl solution for different time and loading condition as shown in **Fig. 7** shows only sign of pitting.

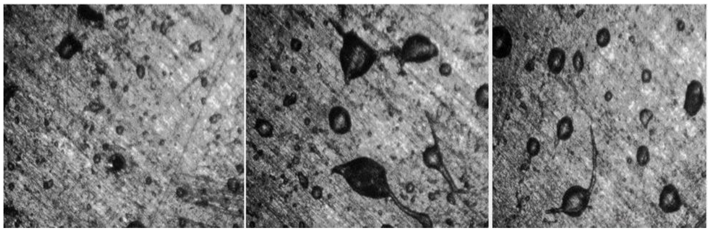

FIGURE 7: Pitting corrosion observed in Salt Spray Specimen

Figure 8.1-8.3, shows that pits size and depth of pits was increased by enhancing the static load from 200 N to 500 N in three different environments such as ambient conditions, distilled water and 3.5% NaCl solution with the different intervals of time i.e. 96 hours, 68 hours, 4.5 hours.

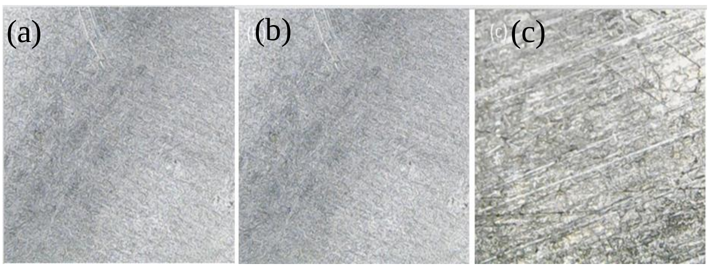

FIGURE 8.1: Optical microscopy images of tensile cross section of Al 6061 T6 samples in open air at constant load of (a)200N (96 hours), (b)500N (68 hours) and (c)800N (4.5 hours) respectively

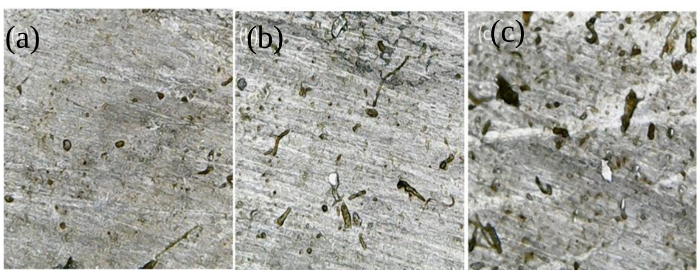

FIGURE 8.2: Optical microscopy images of tensile cross section of Al 6061 T6 samples in distilled water at constant load of (a)200N (96 hours), (b)500N (68 hours) and (c)800N (4.5 hours)

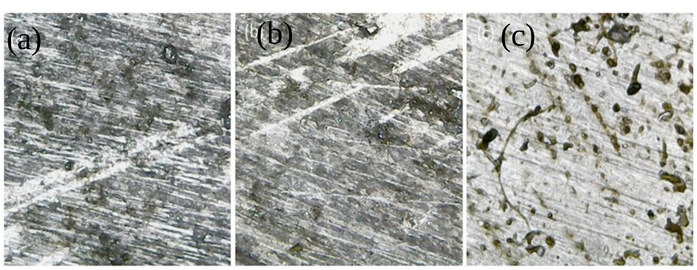

FIGURE 8.3: Optical microscopy images of tensile cross section of Al 6061 T6 samples in 3.5% NaCl solution at constant load of (a)200N(96 hours), (b)500N(68 hours) and (c)800N(4.5 hours)

b. Scanning Electron Microscopy Analysis

Fig 9 shows the SEM micrographs of tensile cross section of Al 6061 T6 when subjected to static load of 200N for 96 hours in open air at different magnification. SEM micrographs clearly depict pitting corrosion which is same as observed in optical micrograph and crack deformation happened in 96hours. Crack propagation can be observed in the sample when load is 200N with loading time 96h but immersed in distilled water environment, as seen in **Figure 10**.

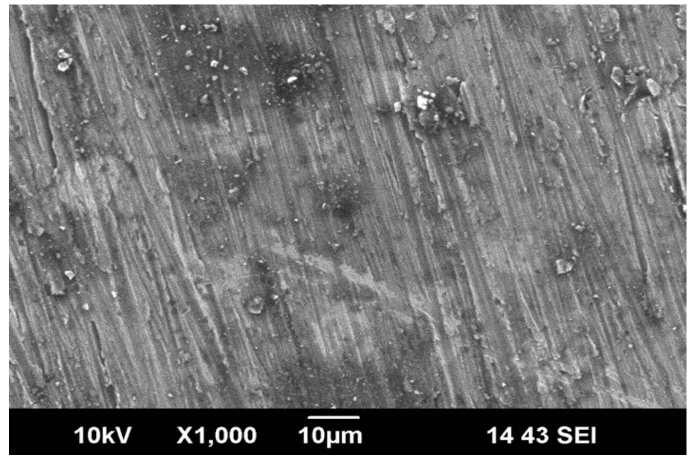

FIGURE 9: Scanning electron fractrograph of Al 6061 T6 sample in open air at static load of 200N for 96 hours at 10μm magnification

In **Fig. 10**, encircled region in the micrograph gave the evidence for the attack at grain boundaries caused by the elemental depletion due to chemical attack or oxidation.

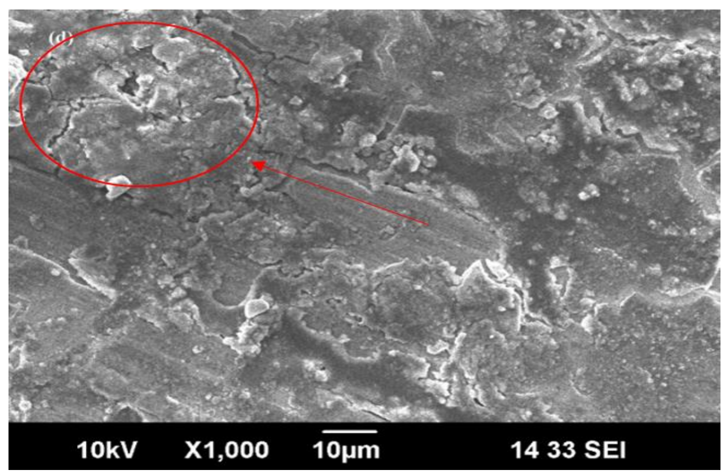

FIGURE 10: Scanning electron fractrograph of Al 6061 T6 sample in distilled water at static load of 200N for 96 hours at 10μm magnification

However, transgranular cleavage like characteristic was found in a sample, which was exposed to 3.5% NaCl solution at a static load of 200N for 96 hours, as shown in **Fig. 11**.

In **Fig. 11**, encircled region in the micrograph again gave the evidence for the attack at grain boundaries caused by the elemental depletion due to chemical attack or oxidation [30-33].

Microstructure changes as in increased load and materials deformed earlier than 200N sample. **Figure 12** shows the SEM images of sample exposed to open air at static load of 500N.

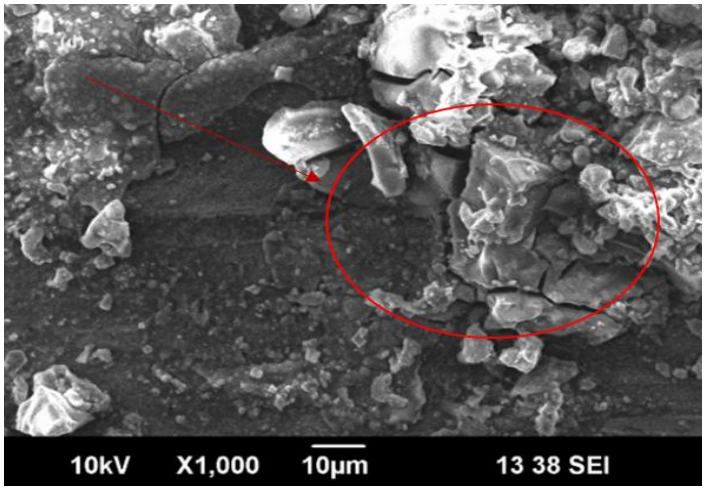

FIGURE 11: Scanning electron fractrograph of Al 6061 T6 sample in 3.5% NaCl solution at static load of 200N for 96 hours at 10μm magnification

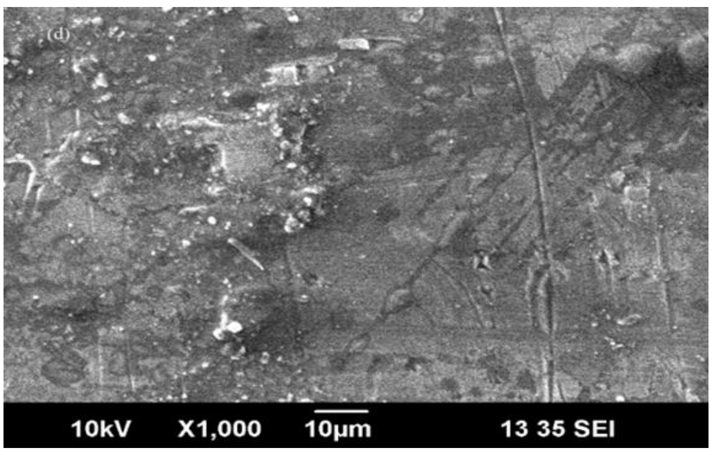

Figure 12 Scanning electron fractrograph of Al 6061 T6 sample in open air at static load of 500N for 68 hours at 10μm magnification

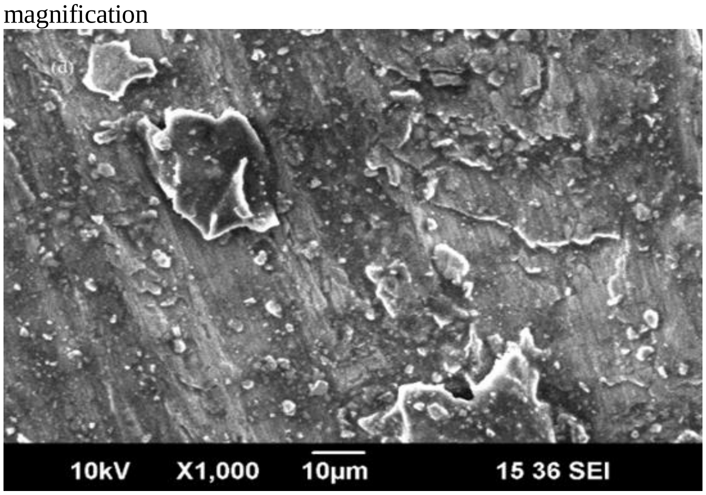

FIGURE 13: Scanning electron fractrograph of Al 6061 T6 sample in distilled water at static load of 500N for 68 hours at 10μm magnification

SEM micrograph in **Fig. 13** evidently represents localized surface corrosion as well as intergranular corrosion when specimen was immersed in distilled water at a constant load of 500N for 68 hours.

SEM micrograph in **Fig. 14** clearly depicts weakening of grain boundaries due to chemical attack of corrosive environment having 3.5% NaCl solution, which results intergranular corrosion.

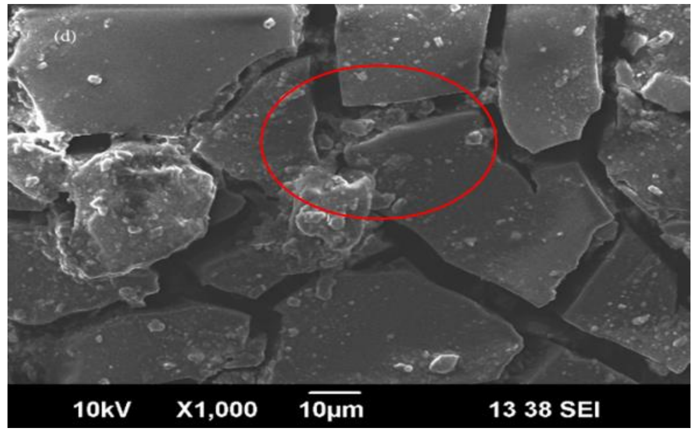

FIGURE 14: Scanning electron fractrograph of Al 6061 T6 sample in 3.5% NaCl solution at static load of 500N for 68 hours at 10μm magnification

Fracture surfaces in **Fig. 15-17** showed dissolution and crack propagation due to anodic grain boundary precipitates. Similar phenomena observed in the peak aged Al-Zn-Mg-Cu-Zr alloy, while the alloy experienced intergranular stress corrosion cracking (IGSCC) [34].

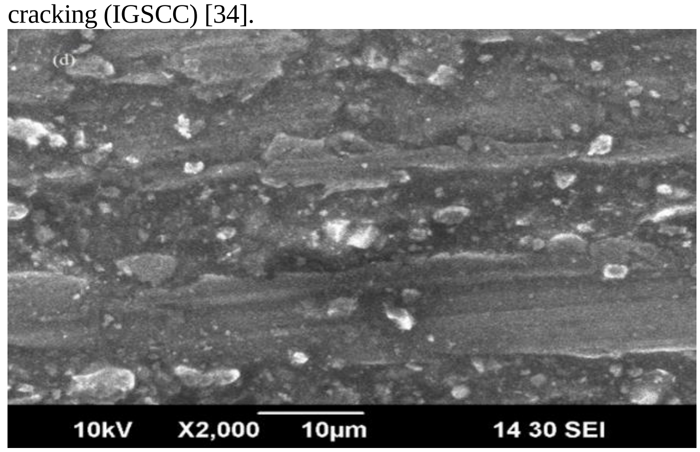

FIGURE 15: Scanning electron fractrograph of Al 6061 T6 sample in open air at static load of 800N for 4.5 hours at 10μm magnification.

V. CONCLUSION

Following conclusions could be drawn from this research work:

1. The specimens subjected to static load of 200N for 96 hours were corroded but minute elongation was observed in distilled water and 3.5% NaCl solution environment.

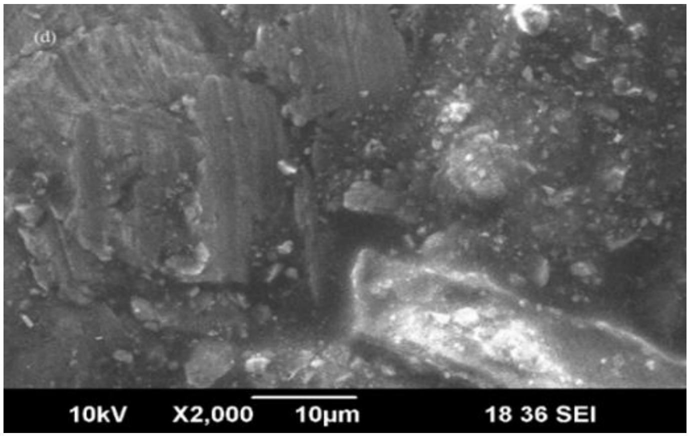

FIGURE 16: Scanning electron fractrograph of Al 6061 T6 sample in distilled water at static load of 800N for 4.5 hours at 10μm magnification

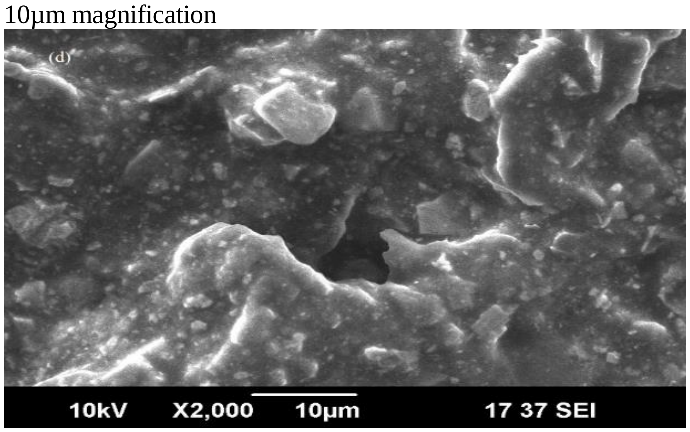

FIGURE 17: Scanning electron fractrograph of Al 6061 T6 sample in 3.5% NaCl solution at static load of 800N for 4.5 hours at 10μm magnification.

2. The specimens under consideration at load of 500N for 68 hours were tarnished but stretched out more than the previous one.
3. More deformation was observed in the samples that subjected to a static load of 800N for 4.5 hours having lower rate of corrosion compared to others.
4. Microstructural analysis gave the evidence of pitting corrosion and cracking.
5. Microstructural analysis also gave the evidence for the attack at grain boundaries caused by the elemental depletion due to chemical attack or oxidation.
6. Weakening of grain boundaries due to chemical attack of corrosive environment results intergranular corrosion.
7. Precipitates and grain boundaries in the present alloy can serve a crack initiation due to hydrogen diffusion.
8. Fractography clearly shows the transgranular fracture as well as intergranular fracture which observed as dimples and extensive ductile tearing.

REFERENCES

[1] J. Hirsch, Recent development in aluminum for automotive applications, T. Nonferrous Met. Soc. 2014, vol. 24, pp. 1995–2002, https://doi.org/10.1016/S1003-6326(14)63305-7.

[2] S Kheirkhah, M Imani , R Aliramezani, M H Zamani and A Kheilnejad, Microstructure, mechanical properties and corrosion resistance of Al6061/BN surface composite prepared by friction stir processing, 2019, https://doi.org/10.1088/2051-672X/ab2a4b

[3] G. W. Stachowiak, Wear: Materials, Mechanisms and Practice, John Wiley & Sons, Ltd, Chichester, England 2006.

[4] FAA, Aviation Maintenance Technician Handbook-General (FAA-H-8083-30A), U.S. Department Of Transportation, Oklahoma 2018, FAA-H-8083-30A), U.S. Department Of Transportation, Oklahoma 2018.

[5] Rao, A. U., Vasu, V., Govindaraju, M., and Srinadh, K. S., "Stress Corrosion Cracking Behaviour of 7xxx Aluminum Alloys: a Literature Review," Trans. Nonferrous Met. Soc. China, 2016, vol. 26, no. 6, pp. 1447–1471.

[6] N. Birbilis, R.G. Buchheit, Electrochemical characteristics of intermetallic phases in aluminum alloys, J. Electrochem. Soc. 2005, vol. 152, pp. B140-B151.

[7] Z. Nikseresht, F. Karimzadeh, M.A. Golozar, M. Heidarbeigy, Effect of heat treatment on microstructure and corrosion behavior of Al6061 alloy weldment, Mater. Des. 2010, vol. 31, pp. 2643-2648.

[8] Zhongqin Tang, Feng Jiang, Mengjun Long, Jingyu Jiang, Huifang Liu, Mengmeng Tong, Effect of annealing temperature on microstructure, mechanical properties and corrosion behavior of Al-Mg-Mn-Sc-Zr alloy, 2020, https://doi.org/10.1016/j.apsusc.2020.14608

[9] Xuehong Xu, Yunlai Deng, Shuiqing Chi, Xiaobin Guo, Effect of interrupted ageing treatment on the mechanical properties and intergranular corrosion behavior of Al-Mg-Si alloys, 2019, https://doi.org/10.1016/j.jmrt.2019.10.050

[10] Mosab Kaseem, Young Gun Ko, Effect of starch on the corrosion behavior of Al-Mg-Si alloy processed by micro arc oxidation from an ecofriendly electrolyte system, 2019, https://doi.org/10.1016/j.bioelechem.2019.04.004

[11] Gaute Svenningsen, Magnus Hurlen Larsen, John Charles Walmsley, Jan Halvor Nordlien, Kemal Nisancioglu, Effect of artificial aging on intergranular corrosion of extruded AlMgSi alloy with small Cu content, Corrosion Science 2006, vol. 48, pp. 1528–1543

[12] T. Ramgopal, P.I. Gouma, G.S. Frankel, Role of grain-boundary precipitates and solute-depleted zone on the intergranular corrosion of aluminum alloy 7150, Corrosion 2002, vol. 58, pp. 687-697.

[13] G. Svenningsen, M.H. Larsen, J.C. Walmsley, J.H. Nordlien, K. Nisancioglu, Effect of artificial aging on intergranular corrosion of extruded AlMgSi alloy with small Cu content, Corrosion Sci. 2006, vol.48, pp. 1528-1543.

[14] W. Zhang, G.S. Frankel, Transitions between pitting and intergranular corrosion in AA2024, Electrochim. Acta 2013, vol. 48, pp. 1193-1210.

[15] T.-S. Huang, G.S. Frankel, Influence of grain structure on anisotropic localized corrosion kinetics of AA7xxx-T6 alloys, Corrosion Eng. Sci. Technol. 2013, vol. 41, pp. 192-199.

[16] Y. Liu, Z. Wang, and W. Ke, Study on Influence of Native Oxide and Corrosion Products on Atmospheric Corrosion of Pure Al, Corros. Sci., 2014, vol. 80, pp. 169–176

[17] B. Wang, Z. Wang, W. Han, and W. Ke, Atmospheric Corrosion of Aluminium Alloy 2024-T3 Exposed to Salt Lake Environment in Western China, Corros. Sci., 2012, vol. 59, pp. 63–70

[18] S. Sun, Q. Zheng, D. Li, and J. Wen, Long-Term Atmospheric Corrosion Behaviour of Aluminium Alloys 2024 and 7075 in Urban, Coastal and Industrial Environments, Corros. Sci., 2009, vol. 51, pp. 719–727

[19] S. Sun, Q. Zheng, D. Li, S. Hu, and J. Wen, Exfoliation Corrosion of Extruded 2024-T4 in the Coastal Environments in China, Corros. Sci., 2011, vol. 53, pp. 2527–2538

[20] H. Li, P. Zhao, Z. Wang, Q. Mao, B. Fang, R. Song, Z. Zheng, The intergranular corrosion susceptibility of a heavily overaged Al-Mg-Si-Cu alloy, Corros. Sci., 2016, vol. 107, pp. 113-122. https://doi.org/10.1016/j.corsci.2016.02.025

[21] D. Elabar, G.R. La Monica, M. Santamaria, F. Di Quarto, P. Skeldon, G.E. Thompson, Anodizing of aluminium and AA 2024-T3 alloy in chromic acid: Effects of sulphate on film growth, Surf. Coat. Technol., 2017, vol. 309, pp. 480-489.

[22] Yilin Sun, Chong Li, Liming Yu, Zhiming Gao, Xingchuan Xia, Yongchang Liu, Corrosion behavior of Al-15%Mg2Si alloy with 1% Ni addition, 2020, https://doi.org/10.1016/j.rinp.2020.103129

[23] Silva, G., Rivolta, B., Gerosa, R., and Derudi, U., “Study of the SCC Behavior of 7075 Aluminum Alloy After one-step Aging at 163 C,” J. Mater. Eng. Perform, 2013, vol. 22, no. 1, pp. 210–214.

[24] N.I.I. Mansor, S. Abdullah, A.K. Ariffin, J. Syarif, "A review of the fatigue failure mechanism of metallic materials under a corroded environment" Engineering Failure Analysis, 2014, vol. 42, pp. 353-365.

[25] Matthew Weber, Paul D. Eason, Hüseyin Özdeş, Murat Tiryakioğlu (2017). "The effect of surface corrosion damage on the fatigue life of 6061-T6 aluminum alloy extrusions" Materials Science & Engineering, vol. 690, pp. 427–432.

[26] K.D. Ralston, D. Fabijanic, N. Birbilis, Effect of grain size on corrosion of high purity aluminium, Electrochim. Acta 2011, vol. 56, pp.1729–1736, https://doi.org/10.1016/j.electacta.2010.09.023.

[27] Meng, C., Zhang, D., Zhuang, L., and Zhang, J., 2016, “Correlations Between Stress Corrosion Cracking, Grain Boundary Precipitates and Zn Content of Al–Mg–Zn Alloys,” J. Alloy. Compd., 655, pp. 178–187.

[28] Knight, S. P., Pohl, K., Holroyd, N. J. H., Birbilis, N., Rometsch, P. A., Muddle,B. C., and Lynch, S. P., 2015, “Some Effects of Alloy Composition on Stress Corrosion Cracking in Al–Zn–Mg–Cu alloys,” Corros. Sci., 98, pp. 50–62.

[29] Holroyd, N.J.H. Environment-Induced Cracking of High-Strength Aluminum Alloys. In Proceedings of the First International Conference on Environmental Induced Cracking of Metals, Sheboygan, WI, USA, 2–7 October 1988; Gangloff, R.P., Ives, M.B., Eds.; National Association of Corrosion Engineers: Houston, TX, USA, 1990; pp. 311–345.

[30] Renner, F.U.; Ankah, G.N.; Bashir, A.; Ma, D.; Biedermann, P.U.; Shrestha, B.R.; Nellessen, M.; Khorashadizadeh, A.; Losada-Pérez, P.; Duarte, M.J.; et al. Star-shaped crystallographic cracking of localized nanoporous defects. Adv. Mater. 2015, vol. 27, pp.4877–4882.

[31] AL-Mangour, B.; Vo, P.; Mongrain, R.; Irissou, E.; Yue, S. Effect of heat treatment on the microstructure and mechanical properties of stainless steel 316L coatings produced by cold spray for biomedical applications. J. Therm. Spray Technol. 2014, vol. 23, pp.641–652.

[32] Liu, X.; Frankel, G.S.; Zoofan, B.; Rokhlin, S.I. In-situ observation of intergranular stress corrosion cracking in AA2024-T3 under constant load conditions. Corros. Sci. 2007, vol.v49, pp. 139–148.

[33] Phull, B. Evaluating stress-corrosion cracking. In ASM Handbook Corrosion: Fundamentals, Testing, and Protection; ASM International: Russell Township, OH, USA, 2003; pp. 42–44.

[34] Lynch S.P. (2003), ‘Mechanisms of hydrogen assisted cracking – a review’ in Hydrogen Effects on Material Behavior and Corrosion Deformation Interactions (Ed. R.H. Jones), Warrendale, PA: The Minerals, Metals and Materials Society (TMS), pp. 449–466